AIMS Bioengineering, 9(2): 145–162.
DOI: 10.3934/bioeng.2022011
Received: 31 January 2022
Revised: 19 March 2022
Accepted: 21 April 2022
Published: 25 April 2022

http://www.aimspress.com/journal/Bioengineering

Research article

An analog electronic circuit model for cAMP-dependent pathway—towards creation of Silicon life

Maria Waqas*, Urooj Ainuddin and Umar Iftikhar

Department of Computer and Information Systems Engineering, NED University of Engineering and Technology, University Road, Karachi - 75270, Pakistan

*** Correspondence:** Email: mariaw@cloud.neduet.edu.pk; Tel: +9221992612618; Fax: +922199261255.

Abstract: Among the most sought after breakthroughs nowadays to combat computational saturation in the electronic hardware realm, neuromorphic and cytomorphic mimetics of biological structures seem potentially promising. Biological circuits are distinguishable due to their minuscule dimensions and immensely low power consumption; yet they achieve extremely complex and magnificent tasks of life, such as, thinking, memorizing, decision making and self-regulating in response to the surroundings. Low power analog circuit solutions are edged over digital ones as they are inherently noisy and fuzzy like bio-systems. In this paper, an analog circuit equivalent for a well-known biological pathway, cyclic adenosine monophosphate (cAMP), has been proposed, exploiting the fabrication characteristics of an analog transistor. The work demonstrates an application of previously published research of the authors, where it was shown that a single transistor operating in analog mode can mimic some fundamental biological circuit processes like receptor-ligand binding, Michaelis Menten and Hill process reactions. Since biological pathways are chain connections of such reactions, same modular approach can be used to build electronic pathways using those basic transistor circuits. Although the idea of creating silicon life seems far-fetched at this stage, this work supplements the idea of cytomorphic chips which is already gaining interest of bio-engineering community.

Keywords: analog circuit mimetics; cAMP pathway; computational biology; cytomorphic hardware design; Michaelis Menten kinetics; receptor-ligand binding

1. Introduction

Since creation of life on earth, computers have been pervasive and ubiquitous. Living systems have enormous computational capabilities that are unmatched to any man-made system till date. None of synthetic electronic machinery has ever been able to outshine the bio-organic computer called human-brain in computational speed, coding capability, storage capacity, power efficiency and massive parallelism. With speed and miniaturization limits on electronic computing machines and Moore's law approaching saturation, many researchers see electronic analog computers mimicking bio-systems as one of the viable alternatives to the traditional digital computers.

Significant efforts in this bio-electronic modeling domain include development of comprehensive analogies among genetic and electronic parameters and processes to convert gene regulation processes into CMOS level equivalent electronic circuits [1–3]. Sequential circuit level designs have also been proposed to model biological processes and cell signaling pathways that can be traversed through in synchronization with the circadian timings [4–6]. Researchers favoring the analog domain have coined the term Cytomorphic hardware meaning bio-inspired electronic hardware and claim that biological systems resemble closer in functionalities to analog systems than digital systems, since many bio-cellular mechanisms work in analog manner rather than strict boolean ON/OFF restriction. They also emphasize that analog equivalent circuits of biological processes are likely to be better in energy efficiency and speed than any digital implementation using very few transistors. Supporting research work includes [7], where less than 12 transistors have been used to emulate higher order kinetic equations, and [8,9], where genetic transcription mechanism found in bacteria has been modeled employing eight transistors only. A thorough review of synthetic bio-circuit designing on silicon substrate using analog transistor devices has been published [10], supplemented with a Cytomorphic chip mimetic of basic bio-molecular circuits [11]. Here the researchers quantitatively mimicked some of the frequently found bio-cellular mechanisms in electronic domain. Most recently electronic circuit software and digitally programmable cytomorphic chips have been used to automate this bio-electronic design process, showing significant progress in rapid prototyping of such circuits which can be used for hierarchical modeling of larger systems [12–19]. Some credible work on noise of such circuits has also been done [20,21]. Some other related efforts include [22–24].

Humble contributions in this domain by the authors of this research work include similar electronic designs involving an alternative modeling technique based on the notion that many bio-chemical structures and processes in the kinetic processes naturally map to some electronic quantities, and utilizing these resemblances can diminish the size of the analogous electronic mimetics drastically, hence mitigating the intricacies involved in cellular processes when holistic view of an entire system is taken [25–27]. The main idea which forms the basis of this research work is that there is a small set of basic bio-chemical reactions that is found recurring in most bio-cellular processes. Devising robust electronic models for these basic processes can help in faster and efficient designing of larger bio-cellular systems. In this paper, the authors have presented one such application, where electronic circuit models of two basic bio-chemical reactions, receptor-ligand binding and Michaelis Menten kinetics, designed in [25], have been used to design a simple but complete second messenger system called cAMP-dependent pathway. The novelty of the work presented in this paper is the analog electronic model equivalence of the mathematical model of cAMP pathway. The results have been analytically and graphically proven. Also, analog electronic equivalence for such a complete bio-process like cAMP pathway is novel in itself. As discussed in the preceding text of this section, previously either individual chemical processes have been modeled or, at higher level like pathways, only digital state machine models have been presented. The work presented in this paper comes under the ambit of applied

sciences, which can be extended and be beneficial in medical sciences as well as engineering. This work can be extremely helpful in drug development. Various research works have proposed electronic counterparts to genetic elements or circuits, with the hope that biological study will one day be ported to the electronic workbench with the help of such incremental contributions. Examples of such works are [1–3,28]. It is evident from these studies that this research has immense value and application in life sciences.

A living cell is an organic computing and response system which is triggered by external stimuli to perform a variety of tasks essential to maintain life. The external stimuli, also called first messengers, are received by receptors situated on a cell membrane, and passed to some second messenger system present inside the cell. These intracellular second messenger systems are cascades of organic molecules, also called pathways, responsible for transporting the stimuli to various parts of the cells. A number of second messenger systems work inside a cell to trigger different type of functions such as gene expression and metabolism. cAMP-dependent pathway is one such second messenger system which plays a vital role in many important biological systems.

1.1. The cAMP-dependent pathway

cAMP (cyclic adenosine monophosphate) is second messenger protein, produced as a result of cAMP-dependent pathway activation. This protein in turn is responsible for mediation of a variety of important life processes such as heart rate relaxation, water absorption in kidneys, breakdown of fat molecules, and maintenance of memory in brain. The proceeding text in this section briefly describes major events that take place in this second messenger cascade [29–32].

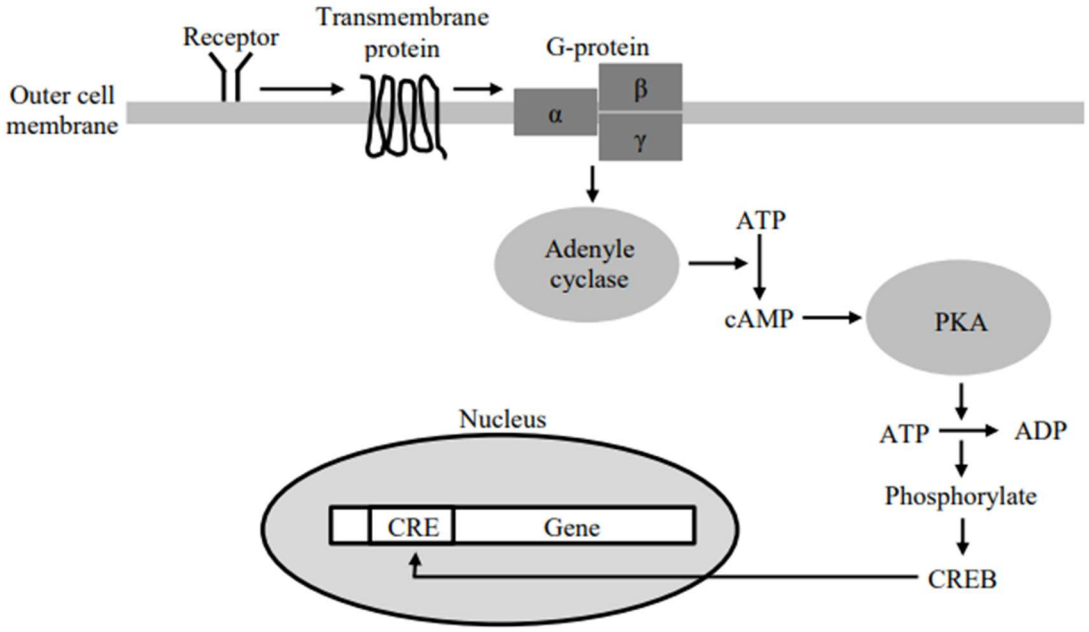

Figure 1. The cAMP-dependent pathway.

Figure 1 provides a figurative description of the cAMP-dependent pathway. It is a secondary messenger system used by many endocrine proteins or hormones to cause an effect in the target cell. These proteins serve as stimuli which bind to receptors present on the cell's outer membrane. A list of such hormone or proteins can be found in [30] and [31]. Different receptors work with different stimuli

protein. The receptor is in turn bound to a transmembrane protein which activates another molecule called G-protein having three subunits called α, β and γ. This activation of G-protein could be inhibitory or stimulatory depending on the type of the receptor. G-protein then turn on an enzyme called adenyl cylase which converts a compound present in the cytoplasm called ATP (adenosine triphosphate) into cAMP. cAMP activates another enzyme called PKA (protein kinase A) along the pathway. The main purpose of a kinase molecule is phosphorylation (addition of phosphate groups) of other proteins. Here it does this by converting ATP molecules into AMP (adenosine monophosphate), freeing two phosphates. These free phosphates are then used to phosphorylate other proteins and enzymes. One such important transcription factor protein as shown in the figure in CREB (cAMP responsive element binding) protein. Once CREB is activated by PKA it diffuses inside the nucleus and binds to a DNA promotor CRE (cAMP response element) to cause gene expression of a particular type.

1.1.1. Role of cAMP-dependent pathway in context of long term potentiation (LTP)

Neurons communicate and process information through both chemical and electrical signals passing through the synapses (passage way structures) between dendrites (sensors) and axons (actuators). However, for information storage, neurons undergo persistent changes in response to these signals. The capacity of nervous system to change is called plasticity and it can affect the structure and function of the entire neural system. It forms the basis of learning and memory [33]. Long term potentiation (LTP) has been considered as the possible phenomenon underlying long lasting changes in synaptic plasticity. The process of LTP can be divided into two major phases. The early phase modifies the existing protein and their trafficking at synapses. Here calcium dependent increase in the number of a specific receptor called AMPA (α-amino-3-hydroxy-5-methyl-4-isoxazolepropionic acid) receptor and their activity takes place. This stage last for about few seconds at most. The late phase involves protein synthesis and gene transcription activated by the transcription factor CREB. As discussed in the preceding text of this section, activation of CREB is done by the cAMP-dependent pathway. This results in the formation of new spines in the dendrite, thus strengthening the synaptic connection [33]. Stronger the connection, more the longevity of the memory. Memories formed this way are expected to be recalled after weeks, or months or even years [34].

2. Materials and methods

2.1. Deterministic mathematical model

As can be seen from the description given in last section, cAMP-dependent pathway is a cascade of similar type of basic bio-chemical reactions each activating the other. These basic bio-chemical reactions fall into two categories; one is simple activation of a molecule by another molecule which could be a reactant or an enzyme – *receptor ligand binding*; and the other is enzymatic reaction, in which an enzyme catalyzes the process of a reactant forming some product – *Michaelis Menten reaction*. Both these processes can be modeled using ordinary differential equations (ODEs), hence a deterministic mathematical model can been devised for the entire process taking place in the cAMP-dependent pathway.

A number of deterministic models have been reported for cAMP-dependent pathway in literature of bio-chemistry and molecular biology. The model adopted in this research work for electronic equivalence has been derived from the work presented in [35], which reports simulation and comparison of several possible models for the reactions taking place in the pathway. The model taken as reference

for this research work is the *simplified cAMP model A* which is a conceptual model of the entire camp pathway.

The overall process of cAMP-dependent pathway can be viewed as a series of four major sub-processes, namely, G-protein activation, adenyl cyclase activation, cAMP production and protein kinase A activation. An external stimuli activates G-proteins; G-proteins then trigger adenyl cyclase molecules which are enzymes; these enzymes in turn catalyzes the production of cAMP from ATP molecules present in the cytoplasm; and finally these cAMP molecules activate protein kinase A molecules. Each of these processes are described and worked for ODEs in the following subsections.

2.1.1. G-protein activation

G-protein activation is a simple receptor-ligand binding process with G-protein acting as the receptor and stimuli acting as the ligand. Equation (1) is the model equation for G-protein activation from inactive state G_i to active state G_a, in response to an external stimuli S. $k_{f_{GP}}$ and $k_{r_{GP}}$ respectively are the forward and reverse rate constants for the reaction.

$$GP_i + S \underset{k_{r_{GP}}}{\overset{k_{f_{GP}}}{\rightleftharpoons}} GP_a \tag{1}$$

Equation (2) shows the deterministic ODE for this process. GP_a and GP_i are the concentrations of active and inactive G-proteins respectively. S represents the concentration of the stimulating molecule. $d[GP_a]/dt$ gives the rate of formation of active G-protein molecules.

$$\frac{d[GP_a]}{dt} = k_{f_{GP}}[GP_i][S] - k_{r_{GP}}[GP_a] \tag{2}$$

The total concentration of G-protein molecules $[totalGP]$ remains conserved throughout the reaction, hence $[totalGP] = [GP_i] + [GP_a]$. Using this, (2) can be written as (3).

$$\frac{d[GP_a]}{dt} = k_{f_{GP}}([totalGP] - [GP_a])[S] - k_{r_{GP}}[GP_a] \tag{3}$$

Defining dissociation constant $K_{d_{GP}}$ for the reaction as $k_{r_{GP}}/k_{f_{GP}}$, (3) can be changed to a final form given in (4).

$$\frac{d[GP_a]}{dt} = \frac{k_{r_{GP}}}{K_{d_{GP}}}([totalGP] - [GP_a])[S] - k_{r_{GP}}[GP_a] \tag{4}$$

After reaching a steady state, production of GP_a becomes negligible, thus $d[GP_a]/dt$ approaches zero. This behavior is represented by (5). The G-protein concentration produced by (4) is then used in the next process of adenyl cyclase activation.

$$[GP_a] = \frac{[totalGP][S]}{K_{d_{GP}} + [S]} \tag{5}$$

2.1.2. Adenyl cyclase activation

Activation of adenyl cyclase molecule is again a receptor-ligand binding process where the G-protein ligand molecules bind to the adenyl cyclase receptors. Equation (6) is the model equation for the reaction where GP_a is the G-protein triggered by the previous process as given in (4). AC_i and AC_a represent the inactive and active adenyl cyclase molecules, whereas $k_{f_{AC}}$ and $k_{r_{AC}}$ are the forward and reverse reaction rate constants respectively.

$$GP_a + AC_i \underset{k_{r_{AC}}}{\overset{k_{f_{AC}}}{\rightleftharpoons}} AC_a \tag{6}$$

Working on the same lines as in previous section, the ODE equation for rate of production of active adenyl cyclase molecules $d[AC_a]/dt$ is given in (7), where $[AC_i]$ and $[AC_a]$ respectively are the concentrations of inactive and active molecules of adenyl cyclase, $[totalAC]$ is equal to $[AC_i] + [AC_a]$, and $K_{d_{AC}}$ is defined as $k_{r_{AC}}/k_{f_{AC}}$.

$$\frac{d[AC_a]}{dt} = \frac{k_{r_{AC}}}{K_{d_{AC}}}([totalAC] - [AC_a])[GP_a] - k_{r_{AC}}[AC_a] \tag{7}$$

The corresponding steady state behaviour is given in (8). The adenyl cyclase molecules produced in this reaction are the enzymes used for cAMP production.

$$[AC_a] = \frac{[totalAC][GP_a]}{K_{d_{AC}} + [GP_a]} \tag{8}$$

2.1.3. cAMP production

cAMP production is a Michaelis Menten process, where the enzyme AC_a produced in the last reaction catalyses the formation of $cAMP$ molecules from the ATP molecules present in the cellular cytoplasm. The reaction is modeled in (9). It is a two stage process; first the free molecules of adenyl cyclase AC_f combine with ATP substrate to form ATP-adenyl cyclase complex $ATPAC$ which then decomposes into free enzyme and the product $cAMP$ molecules. The total concentration of the enzyme remains conserved during the reaction, hence $[AC_a] = [AC_f] + [ATPAC]$.

$$ATP + AC_f \underset{k_{r_{cAMP}}}{\overset{k_{f_{cAMP}}}{\rightleftharpoons}} ATPAC \xrightarrow{k_{cat_{cAMP}}} AC_f + cAMP \tag{9}$$

$k_{f_{cAMP}}$ and $k_{r_{cAMP}}$ respectively are the forward and reverse rate constants for the first reaction. $k_{cat_{cAMP}}$ is the rate constant for the later reaction. Here the overall reaction is represented by two ODEs;

first one for the production of $ATPAC$ complex, and second for the formation of the final product $cAMP$. The ODE equivalent for the first one is given in (10), where $d[ATPAC]/dt$ is the rate of $ATPAC$ complex formation. The square brackets represent the concentration of the respective molecular quantity.

$$\frac{d[ATPAC]}{dt} = k_{f_{cAMP}}[AC_f][ATP] - k_{r_{cAMP}}[ATPAC] - k_{cat_{cAMP}}[ATPAC] \tag{10}$$

Using the enzyme conservation relation (10) can be written as (11).

$$\frac{d[ATPAC]}{dt} = k_{f_{cAMP}}([AC_a] - [ATPAC])[ATP] \; - k_{r_{cAMP}}[ATPAC] - k_{cat_{cAMP}}[ATPAC] \tag{11}$$

Michaelis constant $K_{M_{cAMP}}$ for this enzymatic reaction is equal to $(k_{r_{cAMP}} + k_{cat_{cAMP}})/k_{f_{cAMP}}$, converting (11) to (12).

$$\frac{d[ATPAC]}{dt} = \left(\frac{k_{r_{cAMP}} + k_{cat_{cAMP}}}{K_{M_{cAMP}}}\right)([AC_a] - [ATPAC])$$

$$[ATP] - k_{r_{cAMP}}[ATPAC]k_{cat_{cAMP}}[ATPAC] \tag{12}$$

The $ATPAC$ complex concentration produced in (12) is then used to form the final product of $cAMP$ molecules. The rate of product formation $d[cAMP]/dt$ is shown in (13).

$$\frac{d[cAMP]}{dt} = k_{cat_{cAMP}}[ATPAC] \tag{13}$$

Under steady state assumption, product formation rate $d[cAMP]/dt$ is given in (14). This concentration of $cAMP$ molecules is responsible for activation of protein kinase A molecules.

$$\frac{d[cAMP]}{dt} = k_{cat_{cAMP}} \frac{[AC_a][ATP]}{K_{M_{cAMP}} + [ATP]} \tag{14}$$

2.1.4. Protein kinase A activation

Protein kinase A molecules are activated by $cAMP$. This is another receptor-ligand binding reaction in the cascade with $cAMP$ being the ligand and protein kinase being the receptor. The model reaction is given in (15), where $cAMP$ molecules convert protein kinase A from inactive state PKA_i to active state PKA_a. $k_{f_{PKA}}$ and $k_{r_{PKA}}$ are the forward and reverse reaction rate constants respectively.

$$PKA_i + cAMP \underset{k_{r_{PKA}}}{\overset{k_{f_{PKA}}}{\rightleftharpoons}} PKA_a \tag{15}$$

The ODE equation for rate of formation of active protein kinase A, $d[ATPAC]/dt$ is given in (16), where square brackets represent the respective concentrations, $[totalPKA] = [PKA_i] + [PKA_a]$, and $K_{d_{PKA}} = k_{r_{PKA}}/k_{f_{PKA}}$.

$$\frac{d[PKA_a]}{dt} = \frac{k_{r_{PKA}}}{K_{d_{PKA}}}([totalPKA] - [PKA_a])[cAMP] - k_{r_{PKA}}[PKA_a] \tag{16}$$

The steady state behaviour is depicted in (17).

$$[PKA_a] = \frac{[totalPKA][cAMP]}{K_{d_{PKA}} + [cAMP]} \tag{17}$$

This last product of cAMP-dependent pathway, the Protein kinase A molecules, can be used to phosphorylate any other transcription factor and enzymes as per requirement of the target process.

2.2. Analog circuit equivalent models

2.2.1. Electronic equivalents for receptor-ligand binding and Michaelis Menten reactions

As indicated earlier, this research work is based on previously established electronic equivalents of receptor-ligand binding and Michaelis Menten reaction; this subsection briefly recaps these findings as reported in [25]. In bio-cellular reactions involving receptor-ligand binding, the ligand molecules L bind to receptor molecules R resulting in conformational (shape) change in the later. The receptor could be an enzyme or its regulator, an ion channel, or a gene expression regulator [36]. The reaction results in formation of receptor-ligand RL complex. Figure 2 shows the ODEs governing the reaction (Figure 2(a)) and block diagram of its equivalent analog electronic model (Figure 2(b)) as presented in [25]. k_f and k_r are the rate constants of first order for association and disassociation respectively. $[L]$ and $[R]$ respectively show the unbound molecular concentrations of ligand and receptor, whereas $[RL]$ indicates the receptor-ligand complex concentration. Here K_d is termed as the disassociation constant. $d[RL]/dt$ and $d[L]/dt$ respectively represent the rate of formation of RL complex and receptor concentrations. When the steady state is attained, production rate of receptor-ligand RL complex becomes negligible and its concentration can be viewed at the output of the multiplication unit.

Michaelis Menten reaction is one more commonly found enzymatic reaction exhibited in bio-cellular systems, where substrate molecules S convert in presence of an enzyme E, into product molecules P. Michaelis Menten reaction is a two-part process: first the substrate S binds to enzyme E to form ES complex at k_1 rate; afterwards, one of the two things can happen; ES complex either decomposes back into substrate and free enzyme at k_{-1} reaction rate, or it converts to final product P at k_{cat} reaction rate [37]. Figure 3 shows the ODEs governing the reaction (Figure 3(a)) and block diagram of its equivalent analog electronic model (Figure 3(b)) as presented in [25]. S, E and ES indicate the initial molecular concentration of substrate, free enzyme molecular concentration and enzyme-substrate complex molecular concentration respectively. K_M is the Michaelis constant. $d[S]/dt$, $d[ES]/dt$ and $d[P]/dt$ respectively represent the rate of formation of substrate, ES complex and the final product concentrations. Like receptor ligand reaction, the steady state product formation can be obtained at the output of the multiplier unit.

$$\frac{d[RL]}{dt} = \frac{k_r}{K_d}[L][R_T - RL] - k_r[RL]$$

$$\frac{d[L]}{dt} = k_r[RL] - \frac{k_r}{K_d}[L][R_T - RL]$$

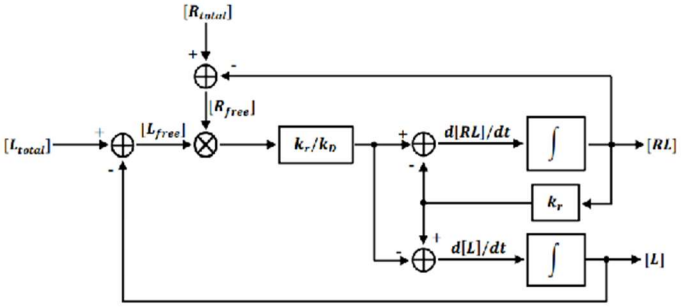

(a) (b)

Figure 2. Deterministic model representations for receptor-ligand binding reaction. (a) ODE representation of the binding reaction. (b) Block diagram depiction of the binding reaction, representing transient as well as steady state mechanisms. [25]

$$\frac{d[S]}{dt} = k_{-1}[ES] - \frac{k_{-1} + k_{cat}}{K_M}[S][E_T - ES]$$

$$\frac{d[ES]}{dt} = \frac{k_{-1} + k_{cat}}{K_M}[S][E_T - ES] - k_{-1}[ES] - k_{cat}[ES]$$

$$\frac{d[P]}{dt} = k_{cat}[ES]$$

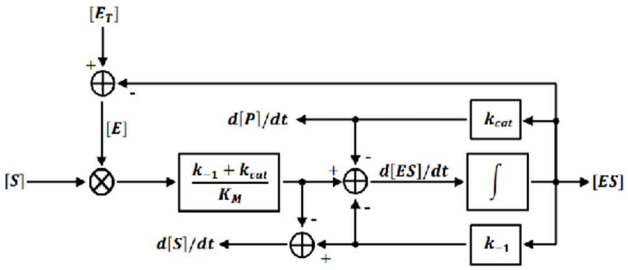

(a) (b)

Figure 3. Deterministic model representations for Michaelis Menten reaction. (a) ODE representation of the reaction. (b) Block diagram depiction of the reaction, representing transient as well as steady state mechanisms. [25]

The novel idea in [25] is that some parameters of bio-cellular entities are analogous to some transistor parameters and exploiting this mapping can reduce the overall size of the electronic counterparts to great extent. One such important analogy is adjusting the disassociation constant K_d of receptor-ligand binding and the Michaelis constant K_M of Michaelis Menten reaction by adjusting length of the transistor. Validation of this analogy and other analogies can be seen in detail in [25]. The publication also contains electronic mimetics for these two bio-reactions based on these analogies. Since these fundamental bio-processes are repeatedly found in bio-cells, these fundamentals electronic circuits can be used to build larger electronic mimetics. cAMP-dependent pathway is one such process which is a cascade of these fundamental processes as described in the previous section.

2.2.2. Proposed analog circuit model for cAMP-dependent pathway

Figure 4 shows the proposed MOS circuit equivalent for the four modules of cAMP-dependent pathway as discussed in the last section. Three of these modules, G-protein activation module, adenyl cyclase activation module and protein kinase A activation module, follow receptor-ligand binding; whereas cAMP production module is based on Michaelis Menten enzymatic reaction. The design of analog MOS electronic circuits for these two bio-chemical reactions have been discussed in the previous

subsection and presented in [25]. These circuits with subtle alterations have been used as sub-modules to build circuit of Figure 4.

Considering Figure 4, for the first sub-module of G-protein activation (the red inset), circuit equivalent of Figure 2(b) have been adopted. $I_{totalGP}$ and I_S are the currents proportional to the initial total concentrations of G-protein and stimuli molecules respectively. These are the external inputs to the circuit supplied from some appropriate current source. V_{GPi} and V_{GPa} are voltages analogous to the concentrations of inactive and active G-protein units. The reverse rate constant k_{rGP} for the reaction is the conductance analogous to $1/R_{krGP}$. The dissociation constant $K_{d_{GP}}$ is represented by the channel length of the nmos transistor (left most) where the input voltage V_{GPi} is applied. The circuit works the same way as described in [25], with R_C, C and R having the same purposes. The current $I_{d[GPa]/dt}$ is equivalent to the rate of production of activated G-protein molecules, which is then integrated to obtain its final output concentration as V_{GPa}. A pmos transistor (right most) has been added at the output which helps in generating current I_{GPa} proportional to $V_{[GPa]}$. This current is then fed to the next sub-module of adenyl cyclase activation as source entity.

The second sub-module of adenyl cyclase activation (the blue inset) is exactly similar to the first module as both reactions are receptor-ligand binding reactions. $I_{totalAC}$ and I_{GPa} are the currents proportional to the initial total concentrations of adenyl cyclase and activated G-protein molecules respectively. $I_{totalAC}$ is externally supplied to the circuit from some appropriate current source, whereas I_{GPa} comes from the previous sub-block. V_{ACi} and V_{ACa} are voltages analogous to the concentrations of inactive and active adenyl cyclase units. The reverse rate constant $k_{r_{AC}}$ for the reaction is the conductance analogous to $1/R_{krAC}$. The dissociation constant $K_{d_{AC}}$is represented by the channel length of the nmos transistor (left most) where the input voltage V_{ACi} is applied. The current $d[AC_a]/dt$ is equivalent to the rate of production of activated adenyl cyclase molecules. Integration of $I_{d[ACa]/dt}$ produces the final concentration of activated adenyl cyclase V_{ACa}, which is in turn converted to a proportional current I_{ACa}. I_{ACa} serves as the source current for the next module of cAMP production.

The third module (the green inset) of Figure 4 is a Michaelis Menten reaction in which the enzyme adenyl cyclase catalyzes the conversion of ATP molecules into $cAMP$ units. This sub-circuit is a slightly modified form of the circuit equivalent given in Figure 3(b), removing the unit used for finding production rate of substrate molecules as this is not needed here. Here the source current I_{ACa} is fed from the last circuit. V_{ATP} is the voltage representing the ATP concentration in the cytoplasm and is set as an external input. This sub-circuit first measures the rate of $ATPAC$ complex formation $I_{d[ATPAC]/dt}$, integrated to find the concentration V_{ATPAC} of the produced $ATPAC$ units. V_{ATPAC} is then used to generate the final current I_{cAMP} which stands proportional to the $cAMP$ concentration produced. V_{ACf} is the concentration of free adenyle cyclase molecules which is used as input to the production unit, the left most nmos transistor having channel length proportional to the Michaelis constant $K_{d_{cAMP}}$. The reverse rate constant $k_{r_{cAMP}}$ for the reaction is the conductance analogous to $1/R_{krcAMP}$. I_{cAMP} is then used as source current for the last subunit for protein kinase A activation.

Protein kinase A activation by $cAMP$ is again a receptor-ligand binding, hence the last module (the purple inset) of Figure 4 is similar to the first two modules in structure and function. Definitions of the differentiating parameters follows. $I_{totalPKA}$ and I_{cAMP} respectively are the currents proportional to the initial total concentrations of protein kinase A supplied from some external current source, and $cAMP$ molecules coming from the last module of $cAMP$activation. V_{PKAi} and V_{PKAa} are voltages analogous to the concentrations of inactive and active protein kinase A units. The reverse rate constant $k_{r_{PKA}}$ for the reaction is the conductance analogous to $1/R_{krPKA}$. The dissociation constant $K_{d_{PKA}}$ is represented by the channel length of the nmos transistor (left most)

where the input voltage V_{PKAi} is applied. The current $I_{d[PKAa]/dt}$ is equivalent to the rate of production of activated protein kinase A molecules, integrated to obtain the final output concentration as V_{PKAa}. V_{PKAa} and its proportional current I_{PKAa} also serves as the final most output of the cAMP-dependent pathway.

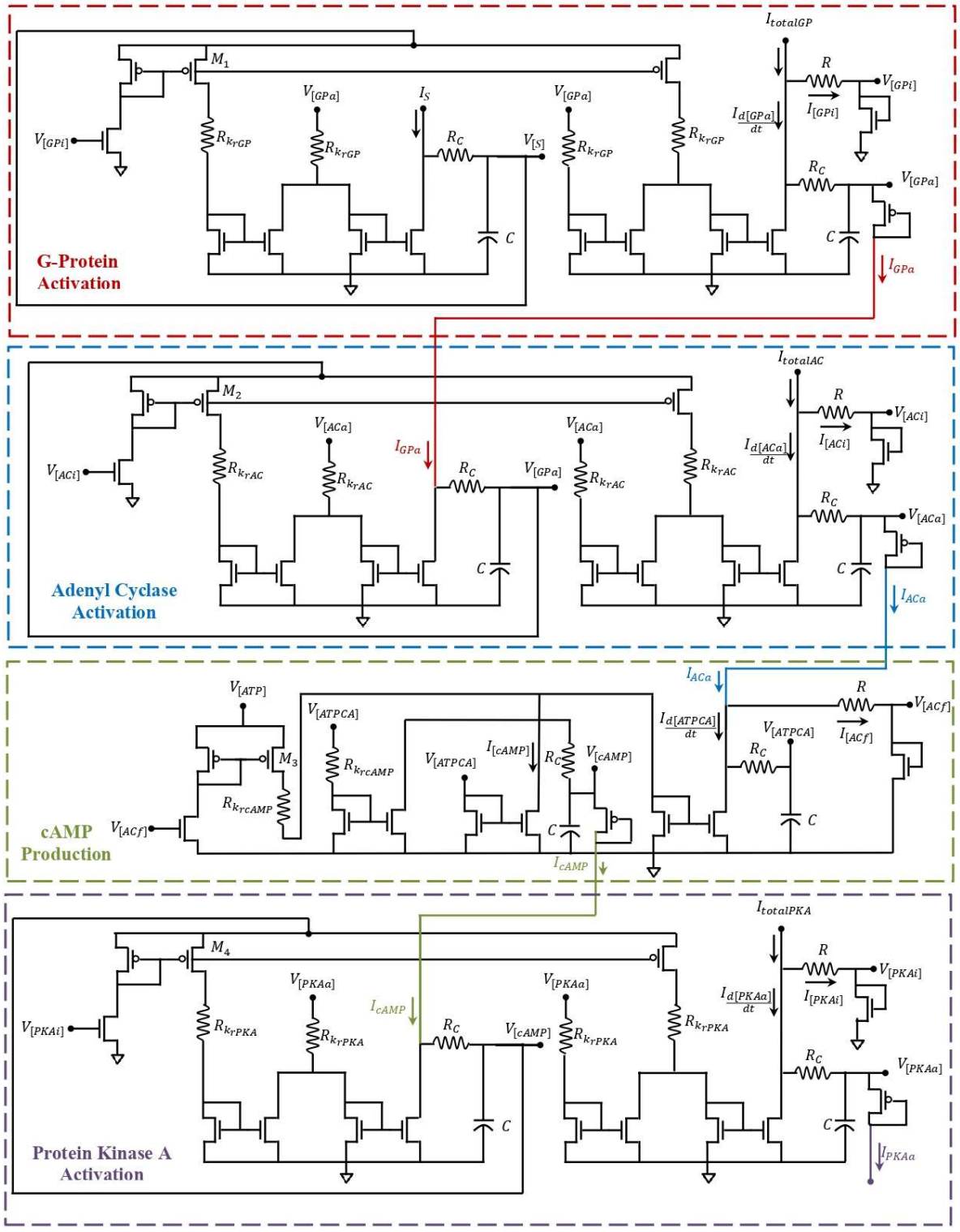

Figure 4. The proposed analog electronic circuit model for cAMP-dependent pathway.

3. Discussion on mathematical analysis of the proposed electronic circuits

In this section, the electronic circuit of Figure 4 has been analyzed to obtain mathematical/electronic equations. These equations reinforce the analogies established among parameters of an electronic transistor and the bio-chemical mechanisms as stated in [25], however there could be many other analogies among the parameters of the two domains which have not been taken into account at this stage in this research endeavor. These mathematically analyzed equations can been plotted using some suitable software and the graphical results for these estimated equations can be validated with the exact plots produced by some electronic design software like Cadence. The parameter values used in the equations can be extracted from Cadence simulations.

Following equations (18) to (21) show approximate electronic behavior mathematically analyzed for the first block, G-Protein Activation (the red inset) of the Figure 4, which has been mapped to the bio-cellular parameters of receptor-ligand binding in the previous sections.

For steady state mechanisms, behaviour of GP_a which is derived from the current at M_1 drain terminal has been estimated as (18), where V_{th} is transistor's threshold voltage, E_{sat} is the critical value of the electrical field at which the saturation of carrier velocity occurs in a transistor and L is the length of the transistor. The rest of the parameters in the equation are cAMP related and have already been described in the previous sections. The form of this equation is analogous to the steady state behavior of G-Protein Activation as shown in (5). The right hand side of (18) actually represents current flowing through M_1, while $[GP_a]$ is the concentration which is analogous to voltage in an electronic circuit, hence the sign of proportionality is used.

$$[GP_a] \propto \frac{(V_{[GPi]} - V_{th})V_{[S]}}{E_{sat}L + V_{[S]}} \frac{1}{R_{krGP}} \tag{18}$$

The proportionality sign can been replaced by MOS transistor device constants as suggested in [25]. Therefore, (18) can be written as (19).

$$[GP_a] = 2C_{ox}Wv_{sat} \frac{(V_{[GPi]} - V_{th})V_{[S]}}{E_{sat}L + V_{[S\}}} \frac{1}{R_{krGP}} \tag{19}$$

Here C_{ox} is the capacitance per unit transistor gate area, W is the width of the transistor and v_{sat} is the saturation velocity. Value for C_{ox} is calculated using (20), whereas E_{sat} is calculated using (21).

$$C_{ox} = \frac{\in_0 \in_r}{T_{ox}} \tag{20}$$

$$E_{sat}L = \frac{V_{dsat}(V_{GPi} - V_{th})}{(V_{GPi} - V_{th}) - V_{dsat}} \tag{21}$$

In (20), $\in_0$ and $\in_r$ respectively are the permittivity of free space and relative permittivity of gate dielectric. T_{ox} is the gate oxide thickness. V_{dsat} is the saturating drain-to-source transistor voltage.

$[GP_i]$ and dGP_a/dt are given in (22) and (23) respectively. Likewise, $[S]$, and $d[S]/dt$ can also be derived from the same circuit, but are not mentioned here as they are of less concern for the next stage in cAMP-dependent pathway. Again, $[GP_i]$ is a concentration value analogous to electronic voltage, hence the sign of proportionality is used. In (23), the effect of RC circuit parameters (R_C and C) have been ignored for simplicity, hence the approximation sign used.

$$[GP_i] \propto I_{totalGP} - I_{\frac{d[GPa]}{dt}} \tag{22}$$

$$\frac{d[GP_a]}{dt} \approx \frac{(V_{[GPi]} - V_{th})V_{[S]}}{E_{sat}L + V_{[S]}} \frac{1}{R_{krGP}} - \frac{V_{[GPa]}}{R_{krGP}} \tag{23}$$

On same lines, the second and the fourth blocks of Figure 4 can also be analysed for electronic behaviour and equivalence. These blocks represent Adenyl Cyclase Activation (the blue inset) and Protein Kinase A Activation (the purple inset) respectively. Following equations (24) to (27) show approximate electronic behaviour for the second stage and equations (28) to (31) show approximate electronic behaviour for the fourth stage of cAMP-dependent pathway. $d[AC_a]/dt$ and $d[PKA_a]/dt$ are currents proportional to the transistor drain current measured at M_2 and M_4 respectively.

$$[AC_a] \propto \frac{(V_{[ACi]} - V_{th})V_{[GPa]}}{E_{sat}L + V_{[GPa]}} \frac{1}{R_{krAC}} \tag{24}$$

$$[AC_a] = 2C_{ox}Wv_{sat} \frac{(V_{[ACi]} - V_{th})V_{[GPa]}}{E_{sat}L + V_{[GPa]}} \frac{1}{R_{krAC}} \tag{25}$$

$$[AC_i] \propto I_{totalAC} - I_{\frac{d[ACa]}{dt}} \tag{26}$$

$$\frac{d[AC_a]}{dt} \approx \frac{(V_{[ACi]} - V_{th})V_{[GPa]}}{E_{sat}L + V_{[GPa\}]} \frac{1}{R_{krAC}} - \frac{V_{[GCa]}}{R_{krAC}} \tag{27}$$

$$[PKA_a] \propto \frac{(V_{[PKAi]} - V_{th})V_{[cAMP]}}{E_{sat}L + V_{[cAMP]}} \frac{1}{R_{krPKA}} \tag{28}$$

$$[PKA_a] = 2C_{ox}Wv_{sat} \frac{(V_{[PKAi]} - V_{th})V_{[cAMP]}}{E_{sat}L + V_{[cAMP]}} \frac{1}{R_{krPKA}} \tag{29}$$

$$[PKA_i] \propto I_{totalPKA} - I_{\frac{d[PKAa]}{dt}} \tag{30}$$

$$\frac{d[PKA_a]}{dt} \approx \frac{(V_{[PKAi]} - V_{th})V_{[cAMP]}}{E_{sat}L + V_{[cAMP]}} \frac{1}{R_{krPKA}} - \frac{V_{[PKAa]}}{R_{krPKA}} \tag{31}$$

The third stage of the pathway is however a bit different as it follows enzymatic Michaelis Menten reaction; it uses the adenyl cyclase produced in second stage to catalyse cAMP production to be used by the fourth stage. Again, using the results reported in [25], (32) to (35) show approximate behaviour mathematically analysed for this stage, the cAMP production stage (the green inset) in Figure 4. Estimated $d[cAMP]/dt$, which stands proportional to the transistor drain current measured at transistor M_3 is shown in (32); other parameters are same as described before.

$$\frac{d[cAMP]}{dt} \propto \frac{(V_{[ACf]} - V_{th})V_{[ATP]}}{E_{sat}L + V_{[ATP]}} \tag{32}$$

Molar concentrations of $ATPAC$ can be calculated using the following equations.

$$[AC_f] \propto I_{ACa} - I_{\frac{d[ATPAC]}{dt}} \tag{33}$$

$$\frac{d[ATPAC]}{dt} \approx \frac{(V_{[ACf]} - V_{th})V_{[ATP]}}{E_{sat}L + V_{[ATP]}} \frac{1}{R_{krcAMP}} - \frac{V_{[ATPAC]}}{R_{krcAMP}} - I_{\frac{d[cAMP]}{dt}} \quad (34)$$

Inserting constants in (32), (35) is obtained.

$$\frac{d[cAMP]}{dt} = 2C_{ox}Wv_{sat}\frac{(V_{[ACf]} - V_{th})V_{[ATP]}}{E_{sat}L + V_{[ATP]}} \quad (35)$$

Here also the value for C_{ox} and E_{sat} are calculated using (20) and (21) respectively.

The equations derived in this sections are similar in structure and parameters to the ones given for deterministic mathematical model or cAMP-dependent pathway, hence the design seems viable when fabricated on an integrated circuit chip.

4. Simulations and results

Steady state behaviour of the whole process, chemical as well as electronic domain, is simulated using Python 3.10.0, run on 64-bit Intel(R) Core i7, 1.8 GHz machine. The values for bio-chemical parameters have been adopted from [35]. $k_{r_{GP}}$ is set to 0.01 s^{-1}, $k_{f_{GP}}$ to 0.1 $mM^{-1}s^{-1}$, $K_{d_{AC}}$ to 1 mM, $k_{cat_{cAMP}}$ to 1 s^{-1}, $K_{d_{cAMP}}$ to 1 mM, $k_{r_{PKA}}$ is set to 0.1 s^{-1}, and $k_{f_{PKA}}$ to 0.1 $mM^{-1}s^{-1}$. Each of $[totalGP]$, $[totalAC]$ and $[PKA]$ is set to $1mM$. The variables $[S]$ and $[ATP]$ are varied from $0mM$ to $10mM$. Figure 5(a) and 5(b) show graphical results of the simulation of these bio-chemical reactions. In Figure 5(a), the blue/dotted line shows the resulting concentrations of $[GP_a]$ against varying $[S]$, the red/solid line shows the resulting concentrations of $[AC_a]$ against $[GP_a]$, and the magenta/dashed line shows the resulting concentrations of $[PKA_a]$ against $[cAMP]$. All concentrations are in mM. Figure 5(b) shows the resulting $cAMP$ production ($d[cAMP]/dt$) in mM/s plotted against the mM concentration of ATP.

For electronic domain simulation, values for transistor design parameters have been adopted from [25]. These are T_{ox} = 7.5 × 10^{-9} m, $\in_0$ = 3.9, $\in_r$ = 8.85 × 10^{-12} F/m, W = 4 × 10^{-6} m, v_{sat} = 95.13 × 10^3 m/s, V_{th} = 562.6 × 10^{-3} V, L = 430 × 10^{-9} m, and V_{dsat} = 224.7 × 10^{-3} V. The value of each of the resistors R_{krGP}, R_{krAC}, R_{krcAMP} and R_{krPKA} is set to 100 Ω. $V_{[GPi]}$, $V_{[ACi]}$, $V_{[ACf]}$ and $V_{[PKAi]}$ are respectively set to 2 V, 3 V, 3 V, and 3 V. Each of $V_{[S]}$ and $V_{[ATP]}$ are varied from 1.5 to 5 V. Figure 5(c) and 5(d) show graphical results of the simulation of the analogous electronic equations. In Figure 5(c), the blue/dotted line shows the resulting concentrations of $[GP_a]$ against varying $[S]$, the red/solid line shows the resulting concentrations of $[AC_a]$ against $[GP_a]$, and the magenta/dashed line shows the resulting concentrations of $[PKA_a]$ against $[cAMP]$. All concentrations are represented as voltages and measured in V. Figure 5(d) shows the resulting $cAMP$ production ($d[cAMP]/dt$) represented as current in mA, plotted against the $[ATP]$ which is measured in V.

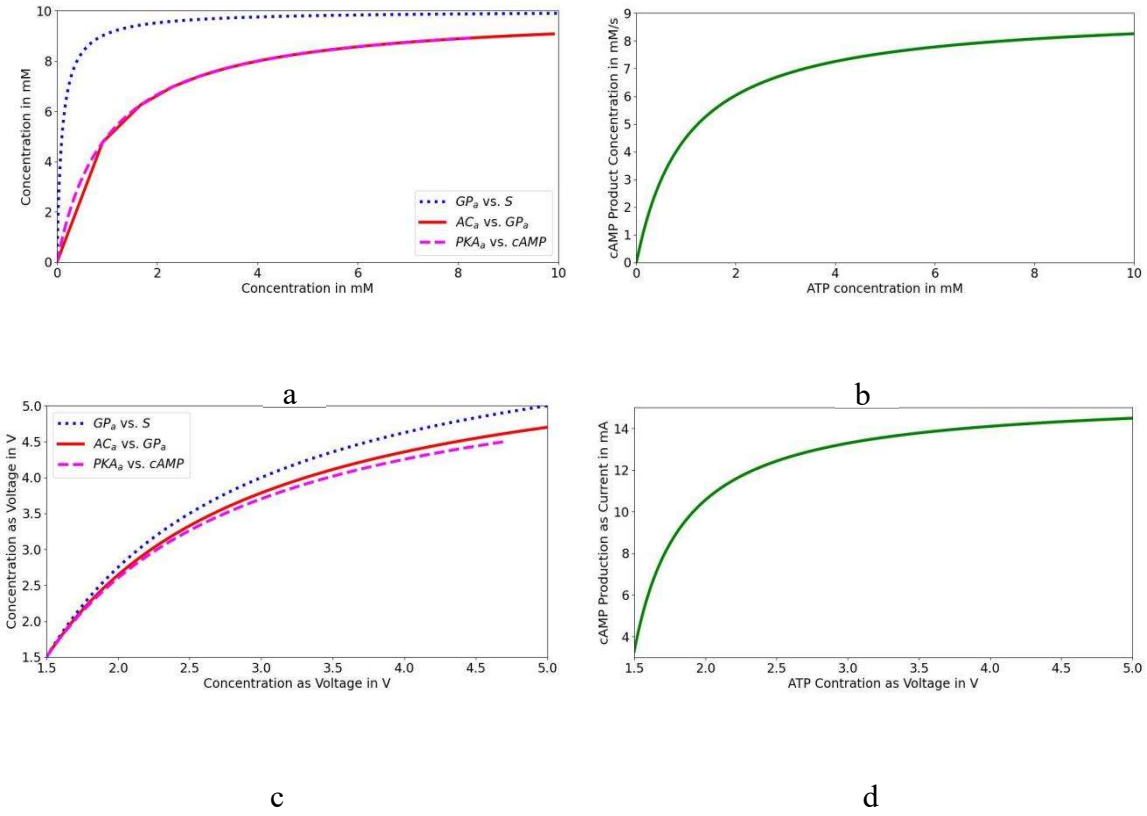

Figure 5. Steady state behaviour of cAMP pathway. (a) Simulation result of bio-chemical domain equations for G-protein activation, adenyl cyclase activation, and protein kinase A activation. (b) Simulation result of bio-chemical domain equation for cAMP production. (c) Simulation result of electronic domain equations for G-protein activation, adenyl cyclase activation, and protein kinase A activation. (d) Simulation result of electronic domain equation for cAMP production.

The plots of Figure 5(a) and 5(c) are analogous and exhibit similar pattern. These plots can be further fine-tuned by simulating the electronic circuit in a more sophisticated electronic integrated circuit design software and extracting the transistor device parameters from it. Due to lack of resources of such software, this work uses these parameters from [25] where similar receptor-ligand binding and Michaelis Menten reaction had been used. Similarly, plots of 5(b) and 5(d) are analogous and are satisfactorily similar.

5. Conclusions

This paper presents an analogous electronic design for the bio-process of cAMP-dependent pathway. Analog circuit modeling on pathway level is the novelty of this work. The deterministic mathematical ODE model of the bio-pathway has been used to derive equivalent electronic mimetic. The resulting equations from the electronic circuit are satisfactorily similar to the bio-chemical equations, resulting in satisfactorily similar simulation results. These results can be further validated through integrated circuit fabrication of the electronic circuit. The simulations would also help mimic and compare timescales of the two domains. The electronic equivalent design of cAMP-dependent pathway presented in this paper is an attempt to validate the basic idea of focusing on modularization

of bio-processes. Likewise other pathways and even larger systems can be modeled efficiently and speedily to produce corresponding electronic mimetics. The development of these biological equivalents in the electronic domain will not only widen the field of mathematical modeling, it will also speed up humanity's move from organism-oriented medicine to cell-oriented medicine.

Conflict of interest

The authors declare no conflict of interest.

Author Contributions:

The first two authors, Maria Waqas and Urooj Ainuddin, contributed equally in the research work and article write-up. The third author, Umar Iftikhar, assisted in write-up and technical finishing of the article.

References

1. Hasan SMR (2008) A novel mixed-signal integrated circuit model for DNA-protein regulatory genetic circuits and genetic state machines. *IEEE T Circuits-I* 55: 1185–1196. https://doi.org/10.1109/TCSI.2008.925632
2. Alam S and Hasan SMR (2013) Integrated circuit modeling of biocellular post-transcription gene mechanisms regulated by microRNA and proteasome. *IEEE T Circuits-I* 60: 2298–2310. https://doi.org/10.1109/TCSI.2013.2245451
3. Rezaul Hasan SM (2010) A micro-sequenced CMOS model for cell signalling pathway using G-protein and phosphorylation cascade. *Int J Comput Appl T* 39: 40–45.
4. Hasan SMR (2010) A digital cmos sequential circuit model for bio-cellular adaptive immune response pathway using phagolysosomic digestion: a digital phagocytosis engine. *J Biomed Sci Eng* 3: 470–475. https://doi.org/10.4236/jbise.2010.35065
5. Ainuddin U and Khurram M (2016) From cell to silicon: Translation of a genetic circuit to finite state machine implementation. *IEEE* 2016: 376–380. https://doi.org/10.1109/INTECH.2016.7845078
6. Ainuddin U, Khurram M, Hasan SMR (2019) Cloning the λSwitch: digital and markov representations. *IEEE T NanoBiosci* 18: 428–436. https://doi.org/10.1109/TNB.2019.2908669
7. Mandal S and Sarpeshkar R (2009) Log-domain circuit models of chemical reactions. *IEEE* 2009: 2697–2700. https://doi.org/10.1109/ISCAS.2009.5118358
8. Mandal S and Sarpeshkar R (2009) Circuit models of stochastic genetic networks. *IEEE* 2009: 109–112. https://doi.org/10.1109/BIOCAS.2009.5372073
9. Daniel R, Woo SS, Turicchia L, et al. (2011) Analog transistor models of bacterial genetic circuits. *IEEE* 2011: 333–336. https://doi.org/10.1109/BioCAS.2011.6107795
10. Teo JJY, Woo SS, Sarpeshkar R (2015) Synthetic biology: a unifying view and review using analog circuits. *IEEE T Biomed Circ* S 9: 453–474. https://doi.org/10.1109/TBCAS.2015.2461446
11. Woo SS, Kim J, Sarpeshkar R (2015) A cytomorphic chip for quantitative modeling of fundamental bio-molecular circuits. *IEEE T Biomed Circ* S 9: 527–542. https://doi.org/10.1109/TBCAS.2015.2446431

12. Achour S, Sarpeshkar R, Rinard MC (2016) Configuration synthesis for programmable analog devices with Arco. *ACM SIGPLAN Notices* 51: 177–193. https://doi.org/10.1145/2980983.2908116
13. Woo SS, Kim J, Sarpeshkar R (2018) A digitally programmable cytomorphic chip for simulation of arbitrary biochemical reaction networks. *IEEE T Biomed Circ* S 12: 360–378. https://doi.org/10.1109/TBCAS.2017.2781253
14. Medley JK, Teo J, Woo SS, et al. (2020) A compiler for biological networks on silicon chips. *PLoS Comput Biol* 16: e1008063. https://doi.org/10.1371/journal.pcbi.1008063
15. Teo JJY, Weiss R, Sarpeshkar R (2019) An artificial tissue homeostasis circuit designed via analog circuit techniques. *IEEE T Biomed Circ* S 13: 540–553. https://doi.org/10.1109/TBCAS.2019.2907074
16. Teo JJY, Kim J, Woo SS, et al. (2019) Bio-molecular circuit design with electronic circuit software and cytomorphic chips. *IEEE* 2019: 1–4. https://doi.org/10.1109/BIOCAS.2019.8918684
17. Teo JJY and Sarpeshkar R (2020) The merging of biological and electronic circuits. *Iscience* 23: 101688. https://doi.org/10.1016/j.isci.2020.101688
18. Zeng J, Banerjee A, Kim J, et al. (2019) A novel bioelectronic reporter system in living cells tested with a synthetic biological comparator. *Sci Rep* 9: 7275. https://doi.org/10.1038/s41598-019-43771-w
19. Zeng J, Teo J, Banerjee A, et al. (2018) A synthetic microbial operational amplifier. *ACS Synth Biol* 7: 2007–2013. https://doi.org/10.1021/acssynbio.8b00138
20. Kim J, Woo SS, Sarpeshkar R (2018) Fast and precise emulation of stochastic biochemical reaction networks with amplified thermal noise in silicon chips. *IEEE T Biomed Circ* S 12: 379–389. https://doi.org/10.1109/TBCAS.2017.2786306
21. Banerjee A, Weaver I, Thorsen T, et al. (2017) Bioelectronic measurement and feedback control of molecules in living cells. *Sci Rep* 7: 12511. https://doi.org/10.1038/s41598-017-12655-2
22. Ahmad W, Rohim RAA, Norhayati Y, et al. (2018) Developing a new dimension of an applied exponential model: application in biological sciences. *Eng Technol Appl Sci Res* 8: 3130–3134. https://doi.org/10.48084/etasr.2124
23. Ahmad W, Aleng NA, Ali Z, et al. (2018) Statistical modeling via bootstrapping and weighted techniques based on variances. *Eng Technol Appl Sci Res* 8: 3135–3140. https://doi.org/10.48084/etasr.2126
24. Ahmad W, Rohim RAA, Ismail NH (2019) Estimate outcome value of doubling cell growth using fuzzy regression method. *Eng Technol Appl Sci Res* 9: 3692–3695. https://doi.org/10.48084/etasr.2467
25. Waqas M, Khurram M, Hasan SM (2017) Bio-cellular processes modeling on silicon substrate: receptor–ligand binding and Michaelis Menten reaction. *Analog Integr Circ S* 93: 329–340. https://doi.org/10.1007/s10470-017-1044-x
26. Waqas M (2019) Integrated circuit models of bio-cellular networks [PhD thesis]. NED University of Engineering & Technology, Karachi. http://173.208.131.244:9060/xmlui/handle/123456789/5232
27. Waqas M, Khurram M, Hasan SMR (2020) Analog electronic circuits to model cooperativity in hill process. *Mehran Univ Res J Eng Technol* 39: 678–685. https://doi.org/10.22581/muet1982.2004.01

28. Zhu Y, Li Y, Zeng N, et al. (2012) Design and analysis of genetic regulatory networks with electronic circuit ideas. *IEEE* 2012: 2046–2049. https://doi.org/10.1109/ICICEE.2012.544
29. Berridge MJ (2007) *Cell Signalling Biology: Module 2 Cell Signalling Pathways*, Portland Press.
30. Berridge MJ (2007) *Cell Signalling Biology: Module 1 Introduction*, Portland Press.
31. Alberts B, Johnson A, Lewis J, et al. (2002) *Molecular Biology of the Cell*, New York: Garland Science, Taylor and Francis Group.
32. Lehninger AL (2004) *Lehninger Principles of Biochemistry: David L. Nelson, Michael M. Cox*, New York: Recording for the Blind & Dyslexic.
33. Mayadevi M, Archana GM, Prabhu RR, et al. (2012) Molecular mechanisms in synaptic plasticity, In: Contreras CM, *Neuroscience-Dealing With Frontiers*, Croatia: IntechOpen, 295–330. https://doi.org/10.5772/36928
34. Alberini CM (2009) Transcription factors in long-term memory and synaptic plasticity. *Physiol Rev* 89: 121–145. https://doi.org/10.1152/physrev.00017.2008
35. Williamson T, Schwartz JM, Kell DB, et al. (2009) Deterministic mathematical models of the cAMP pathway in Saccharomyces cerevisiae. *BMC Syst Biol* 3: 70. https://doi.org/10.1186/1752-0509-3-70
36. Boyle J (2005) Lehninger principles of biochemistry: Nelson, D., and Cox, M. *Biochem Mol Biol Educ* 33: 74–75. https://doi.org/10.1002/bmb.2005.494033010419
37. Berg JM, Tymoczko JL, Stryer L (2002) The Michaelis-Menten model accounts for the kinetic properties of many enzymes. *Biochemistry* 5: 319–330.

AIMS Press